J. Membrane Biol. 63, 157–163 (1981)

The Journal of
Membrane Biology

Time Course of Active Na Transport and Oxidative Metabolism Following Transepithelial Potential Perturbation in Toad Urinary Bladder

Stanley J. Rosenthal, John G. King, and Alvin Essig

Department of Physiology, Boston University School of Medicine, Boston, Massachusetts 02118 and
Department of Physics, Massachusetts Institute of Technology, Cambridge, Massachusetts 02139

Summary. The use of an Ussing chamber with well-defined mixing characteristics coupled to a mass spectrometer permits the concurrent evaluation of transepithelial current and oxidative metabolism with improved temporal resolution. The time-course of the amiloride-sensitive current I^a and the rate of suprabasal CO_2 production $J^{sb}_{CO_2}$ were observed in 10 toad urinary bladders at short-circuit and after clamping $\Delta\psi$ at 100 mV, serosa positive. Following perturbation of $\Delta\psi$ (0→100 mV), I^a declined sharply within 1/2 min, remained near constant ~15 min, and then increased slightly. $J^{sb}_{CO_2}$ declined more gradually, remained near constant at ~4–7 min, and then declined further. Detailed analysis revealed an early quasi-steady state with near constancy of $J^{sb}_{CO_2}$ starting at 2.9 ± 1.1 (SD) min and lasting 4.7 ± 1.8 (SD) min, followed by relaxation to a later steady state at about 15 min. During the early quasi-steady state, I^a was also nearly constant. Considering that in steady states $I^a/F \simeq J^a_{Na}$, the rate of transepithelial active Na transport, during the early quasi-steady state mean values ± SE of J^a_{Na}, $J^{sb}_{CO_2}$ and $(J^a_{Na}/J^{sb}_{CO_2})$ were, respectively, $29.9 \pm 1.7\%$, $59.4 \pm 3.2\%$, and $56.4 \pm 5.7\%$ of values at short-circuit. Corresponding values during the late steady state were $41.4 \pm 6.0\%$, $38.2 \pm 6.1\%$, and $111.3 \pm 8.6\%$. Thus the flow ratio $J^a_{Na}/J^{sb}_{CO_2}$ was depressed significantly during the early quasi-steady state, but returned later to the original value. The results of measurements of I^a and $J^{sb}_{O_2}$ in three hemibladders were qualitatively similar. In terms of a phenomenological "black-box" treatment the findings are consistent with earlier studies indicating incomplete coupling between transport and metabolism. Further studies will be required to clarify the molecular basis for these observations.

Key words: Active transport, oxidative metabolism, toad bladder

The systematic analysis of active transport requires the concurrent measurement of rates of transport and metabolism under diverse conditions. Although steady-state relationships between these processes are well defined, there are important problems in the study of transient behavior necessary to characterize system parameters. For the case of transepithelial active Na transport, since no adequate method exists for simultaneously monitoring transport and the utilization of ATP believed to drive the Na pump, metabolism is commonly evaluated by measurements of the rate of O_2 uptake [2, 14–16, 22, 23, 30] or CO_2 release [1, 4, 6, 7, 13]. Such studies suffer from the difficulty that abrupt changes in transport rate are associated with transients in gas concentration, complicating the prompt evaluation of rates of oxidative metabolism.

We have recently described an apparatus in which well-defined mixing characteristics of an Ussing chamber coupled to a mass spectrometer permit the concurrent measurement of transepithelial current and the rate of oxidative metabolism with improved temporal resolution [25]. We have now employed this apparatus to characterize the time response of the electrical current and O_2 and CO_2 fluxes when the transepithelial electrical potential in the toad urinary bladder is perturbed. The results help to define the dynamic relationship between transepithelial active Na transport and oxidative metabolism [1, 4, 5, 13–16], facilitating a consistent formal treatment.

Materials and Methods

Our technique for monitoring transport and metabolism employs a mass spectrometer to measure CO_2 and O_2 fluxes from a voltage-clamped tissue. The details are given in reference [25].

Briefly, a modified Ussing chamber supports 7.1 cm^2 tissue (female toad urinary bladder, Dominican Republic, National Reagents, Inc., Bridgeport, CT), continuously perfused with aerated

0022-2631/81/0063-0157 $01.40
© 1981 Springer-Verlag New York Inc.

phosphate-Ringer's solution (in mM: Na, 119; K, 3.5; Ca, 0.9; Cl, 118; HPO_4, 2.4; H_2PO_4, 0.57; pH 7.2; 220 mOsm/Kg) containing 40 mg/liter gentamicin sulfate to retard bacterial growth. A high-speed micro-pump drives the solution across the tissue, minimizing the unstirred water layer. The total volume of solution in the chamber and pump is 6 ml.

CO_2 Mode

The effluent of the Ussing chamber is interfaced to a vacuum chamber by a thin Teflon membrane. Molecules entering the vacuum are ionized and filtered according to their mass by a quadrupole mass spectrometer. With the spectrometer tuned to mass 44, the signal is proportional to the CO_2 concentration in solution at the interface. By taking into account flow rate and volume capacity factors, we compute the instantaneous CO_2 efflux rate J_{CO_2} at 6-sec intervals, using a Hewlett Packard 2821 desk computer and the conversion described in [25] for this purpose. At experimental flow rates, the minimum detectable change in J_{CO_2} was 5 pmol/sec with a time resolution of 1 to 2 min, depending on the noise contributed by physical instability of the tissues.

O_2 Mode

Sampling both the influent and effluent and tuning the spectrometer to mass 32 allows the differential measurement of O_2 consumption rates, J_{O_2}. The minimum detectable change in J_{O_2} was 11 pmol/sec, due to the effects of high background noise at ambient pO_2 levels.

Standard voltage-clamping techniques are used to measure the total transepithelial current I at different settings of the transepithelial potential difference $\Delta\Psi$ [30]. At the end of each experiment, 7×10^{-5} M amiloride (Merck, Sharp and Dohme, NJ) was applied to the mucosal surface in order to block Na entry and reduce the metabolic flux rate J_r (r refers to O_2 or CO_2) to its basal level J_r^b; pulses of ±10 mV applied for 10 sec then permitted the calculation from Ohm's law of the "passive conductance" κ^p [15]. (The use of a flow-through system necessitated the further addition of small doses of amiloride at about 8-min intervals in order to maintain depression of function.) Previous studies have demonstrated that, following equilibration, κ^p, $J_{O_2}^b$, and $J_{CO_2}^b$ are near-constant for extended periods and, on abolition of net Na transport with amiloride, are unaffected by perturbation of $\Delta\psi$ over a wide range [10, 13–15].

Accordingly, we computed the time course of the amiloride-sensitive current,

$$I^a \equiv I + \kappa^p(\Delta\Psi), \tag{1}$$

the rate of suprabasal metabolism,

$$J_r^{sb} = J_r - J_r^b, \tag{2}$$

and the dimensionless ratio $I^a/F\ J_r^{sb}$ (F being the Faraday constant).

Results are presented as the mean value ± the standard error (SE) or the standard deviation (SD), as appropriate. Confidence probabilities of differences ($p(\Delta)$) are derived from a Student's t-distribution [28].

Results

In the studies of 18 hemi-bladders transepithelial current I and bathing solution CO_2 concentration were monitored continuously while regulating the transepithelial potential difference $\Delta\psi$. Following a period of at least 1 hr, during which the function of the tissue and the apparatus became stable [25], $\Delta\psi$ was clamped to zero for at least 1 hr. Measurements made during the last 10 min of this period are taken to characterize the initial short-circuit state. $\Delta\psi$ was then set to +100 mV (serosa positive) for periods of 30 to 50 min. Amiloride was then added and the tissue was short-circuited in order to determine active transport-independent activities.

Tissues were considered undamaged if the final value of κ^p was below 1.0 mS and the ratio of κ^p to total conductance κ at short-circuit was below 0.5. In addition, two tissues were discarded because abrupt changes in the CO_2 data (probably due to tissue movement) made calculations of $J_{CO_2}^{sb}$ impossible. The results for the 10 tissues which remained are described below. In order to enhance the activity of four of these tissues with low initial current, aldosterone was added at 5×10^{-7} M at least 1 hr before the stabilization period. The behavior of these tissues was not significantly different from that of the others.

The mean open-circuit potential was 102 ±25 (SD) mV just prior to clamping. The mean κ^p/κ at short circuit was 0.31 ± 0.13 (SD). The mean values of short-circuit current I_0, $J_{CO_2}^{sb}$, and $I^a/FJ_{CO_2}^{sb}$ during the last 10 min of short-circuiting are given in Table 1.

The average time courses of I^a and $J_{CO_2}^{sb}$ for the 10 tissues are shown in Fig. 1. Here each variable in each tissue was normalized to have a mean value of 100% during the final 10-min of the short-circuit period. Average values taken at 1/2-min intervals were then plotted against time. Thus the temporal behavior of each tissue is equally weighted.

With the perturbation of $\Delta\psi$ from 0 to 100 mV (serosa positive) the current I^a dropped sharply to a near steady-state value within 1/2 min, changing only slightly ($<1\frac{1}{2}$% per min) thereafter. The average value of $J_{CO_2}^{sb}$ began to drop immediately after hyperpolarization and flattened out at about 4 min, remaining near constant until about 7 min. Thereafter $J_{CO_2}^{sb}$ dropped more gradually, reaching a final stable value by some 15 min.

In order to analyze the early response more precisely we then considered each tissue individually, determining the first period in which J_{CO_2} becomes approximately constant for at least 1 min. Specifically, we define a plateau as a period longer than 1 min bounded by equal values of J_{CO_2}; the complete plateau is considered to extend to the final time this value is achieved. Fig. 2 shows $J_{CO_2}^{sb}$ and I^a during the first plateau in each tissue. The time course in the tissues differed, with the onset varying from 1.0

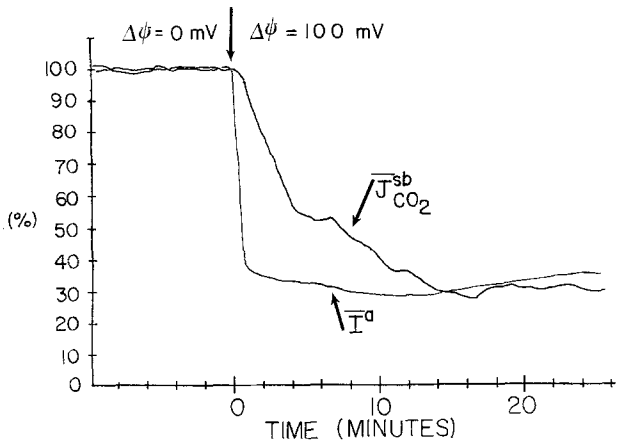

Fig. 1. Average time dependence of I^a and $J^{sb}_{CO_2}$ after polarization at $t=0$ to 100 mV (serosa positive) in 10 tissues. Values were normalized to 100% at short-circuit (mean of time −10 to 0 min). Averages were computed and plotted at 30-sec intervals

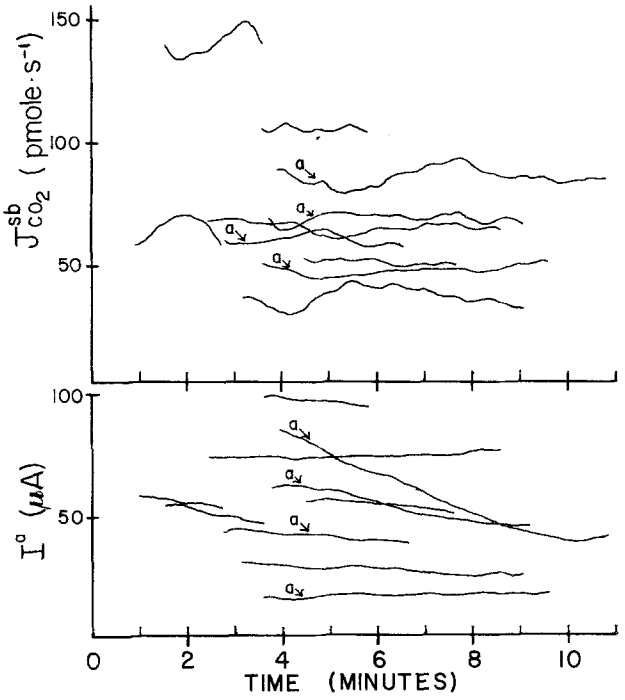

Fig. 2. $J^{sb}_{CO_2}$ and I^a values during the early plateau of each tissue. The letter *a* indicates tissues to which aldosterone has been added

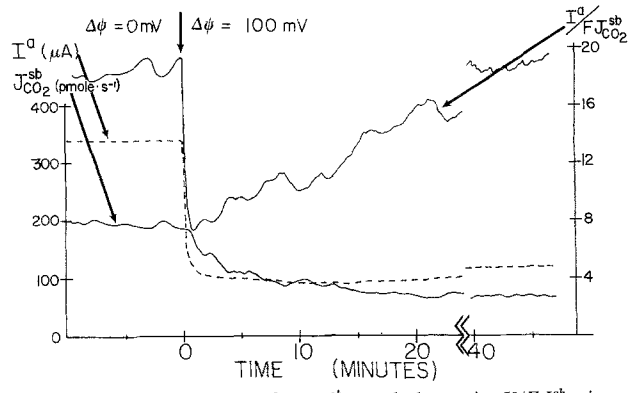

Fig. 3. Time dependence of I^a, $J^{sb}_{CO_2}$ and the ratio $I^a/FJ^{sb}_{CO_2}$ in a typical tissue as calculated at 6-sec intervals. The transepithelial potential was changed from 0 to 100 mV (serosa positive) at $t=0$ min

to 4.8 min (mean 2.9 ± 1.1 (SD) min) and the duration ranging from 2.0 to 6.5 min (mean 4.7 ± 1.8 (SD) min). To characterize the flatness of the plateaus we calculated the average coefficient of variation based on values sampled every 30 sec. This was 4.1 ± 0.6 (SE) %.

Similarly, I^a during the same periods showed a coefficient of variation of 6.5 ± 2.4 (SE) % (if one atypical tissue is deleted this becomes 4.2 ± 0.9 (SE) %).

The simultaneous and frequent measurements of I^a and $J^{sb}_{CO_2}$ allow one to compute the ratio $I^a/FJ^{sb}_{CO_2}$ in a near-continuous fashion. (In the steady state I^a/F equals the rate of transepithelial active Na transport J^a_{Na} [18, 31]; its significance during transient periods will be considered below.) Fig. 3 shows a plot of I^a, $J^{sb}_{CO_2}$ and $I^a/FJ^{sb}_{CO_2}$ for a typical tissue.

The mean values of these parameters from 10 tissues throughout the early plateau, the period 10 to 15 min following hyperpolarization, and the final 10 min of the experiment are indicated in Table 1 as percentages of their values in the initial short-circuit state. The significance of changes was evaluated by paired analyses for each tissue. It is notable that in association with the changes in I^a and $J^{sb}_{CO_2}$ described above the ratio $I^a/FJ^{sb}_{CO_2}$ decreased significantly between the short-circuit period and the early plateau ($\Delta = -43.6 \pm 5.7$ (SE) %, $p(\Delta) < 0.001$). The ratio increased significantly between the early plateau and the 10–15 min period ($p(\Delta) < 0.01$) and between the 10–15 min and final periods ($p(\Delta) < 0.05$); the ratio during the two latter periods was not significantly different from that in the short-circuit period.

Because of various uncertainties concerning the evaluation of oxidative metabolism from CO_2 fluxes, we also measured O_2 fluxes in a few tissues. Since the noise observed on the O_2 signal is some 2 to 3 times greater than that on the CO_2 signal, as explained in Materials and Methods, measurements in this mode were more difficult. Nevertheless, three experiments were acceptable; these demonstrated the same qualitative behavior as in the CO_2 study: an early plateau was discernible in each case. Plateaus commenced 3–6.5 min following perturbation of $\Delta\psi$ and lasted 3.5–5 min. Fig. 4 is a plot of average normalized I^a and $J^{sb}_{O_2}$ of these tissues. Mean normalized values of I^a, $J^{sb}_{O_2}$, and $I^a/FJ^{sb}_{O_2}$ are shown in Table 1. Oxygen experiments were terminated after 20 min; hence the "final period" refers to the period 10 to 20 min following hyperpolarization. The value

Table 1. Mean values of I^a, J_r^{sb} and I^a/FJ_r^{sb} during various periods[a]

	Absolute value at short-circuit ± SD	Normalized value after perturbation ± SE		
		Early plateau (4.7 ± 1.8 (SD) min)	10–15 min period	Final 10 min period
CO_2 ($n=10$)	I^a(176 ± 70 μA)	29.9 ± 1.7%	28.0 ± 2.0%	41.4 ± 6.0%
	$J^{sb}_{CO_2}\left(127 \pm 48 \frac{\text{pmole}}{\text{sec}}\right)$	59.4 ± 3.2%	34.6 ± 3.1%	38.2 ± 6.1%
	$I^a/FJ^{sb}_{CO_2}$(14.7 ± 3.2)	56.4 ± 5.7%	88.4 ± 7.7%	111.3 ± 8.6%
		Early plateau (4.3 ± 0.7 (SD) min)		
O_2 ($n=3$)	I^a(124 ± 36 μA)	21.6 ± 5.1%		20.1 ± 4.3%
	$J^{sb}_{O_2}\left(203 \pm 17 \frac{\text{pmole}}{\text{sec}}\right)$	41.8 ± 10.2%		30.8 ± 9.8%
	$I^a/FJ^{sb}_{O_2}$(6.1 ± 1.4)	57.5 ± 6.3%		87.3 ± 14.3%

[a] Values after +100 mV perturbation were normalized with respect to the average value of the quantity during the last 10 min of short-circuiting prior to the perturbation. The final period for the CO_2 data began at a mean time of 35.0±9.2 (SD) min after the perturbation.

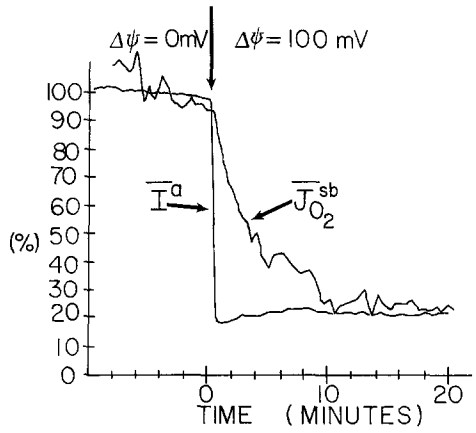

Fig. 4. The average time dependence of I^a and $J^{sb}_{O_2}$ in 3 tissues. Computations and protocol are the same as for Fig. 1

of $I^a/FJ^{sb}_{O_2}$ decreased significantly during the early plateau ($p(\Delta)<0.025$) with a percentage change close to the CO_2 value. Again as in the CO_2 study, the ratio in the final period was indistinguishable from that measured initially at short-circuit.

Discussion

Precise characterization of dynamic aspects of transport and the associated metabolism is fundamental to the elucidation of both thermodynamic and mechanistic aspects of transepithelial active sodium transport. While analysis of molecular events in fine temporal detail must await the development of appropriate techniques, the consideration of quasi-steady states should facilitate formal phenomenological analysis, treating the epithelium as a black box. Pending more precise knowledge of the system, such analysis should be of use in the design and interpretation of experiments. In taking such an approach, however, it is important to consider both technical and conceptual difficulties which may lead to ambiguity in the interpretation of transient phenomena.

In the Dominican Republic toad urinary bladder, Na^+ tracer studies have demonstrated that under appropriate conditions the amiloride-sensitive current I^a reliably evaluated the rate of transepithelial active Na transport in both short-circuited and nonshort-circuited tissues [18, 31]. This equivalence has been demonstrated, however, only ≧10–20 min following voltage-clamping. Furthermore, given the evidence that the apical plasma membrane is permeable essentially only to Na^+, while the basal-lateral membrane is appreciably permeable also to K^+ and Cl^- [19, 20], although soon after perturbation of $\Delta\psi$ the electric current across the two membranes will be the same, for some time the rates of Na flow across the two surfaces must differ [32]. During this period of nonconservative Na^+ flow, while I^a will evaluate the rate of passive apical Na^+ flow, it cannot be assumed to evaluate precisely the rate of active Na^+ transport J^a_{Na} at the basal-lateral surface. The available data do not yet permit precise evaluation of the duration or magnitude of this discrepancy.

There are also important problems in the characterization of the dynamic response of metabolism. For this purpose, lacking a suitable method for

measuring the rate of utilization of ATP, it is common to monitor oxidative metabolism, presumably reflecting oxidative phosphorylation. In well-established steady states the rate of O_2 uptake (or CO_2 release) is constant, both in the absence and presence of amiloride, permitting estimation of the rate of suprabasal O_2 consumption (or CO_2 production) J_r^{sb} associated with the transport process [15, 17]. Again, however, there are ambiguities in interpreting the response to perturbation. Apparently the stimulus for alteration in the rate of oxygen consumption in these circumstances is alteration of the [ATP]/[ADP] $[P_i]$ ratio ("phosphate potential") consequent to altered rates of ATP utilization for active transport [24]. Ideally it would be desirable to monitor mitochondrial oxygen consumption closely in order to define precisely the kinetics of the interaction between transport and metabolism. In practice the precision of measurements is limited by the capacity of the system. In order for the rate of change of bathing solution O_2 or CO_2 concentration to be used to evaluate altered rates of mitochondrial metabolism, it is necessary to achieve a steady state for diffusion of the gases across intracellular structures and the serosal limiting membrane, as well as poorly stirred extracellular compartments. In addition to precluding rapid kinetic studies of *in situ* mitochondrial function, such delay, if sufficiently long, may interfere also with characterization of epithelial steady-state behavior, since prolonged perturbation of driving forces in an attempt to quantify system parameters may alter the very parameters which it is desired to evaluate. The significance of this consideration is indicated by earlier observations in the frog skin. In this tissue, perturbation of $\Delta\psi$ for 15 min or longer produced a "memory effect", such that subsequent values of the short-circuit current and the associated rate of O_2 consumption differed appreciably from values measured at short-circuit prior to perturbation [30]. In such circumstances prolonged perturbations are unlikely to permit reliable estimates of the voltage-dependence of current or metabolism.

In previous studies of the voltage dependence of Na transport and O_2 comsumption in anuran epithelia, in an attempt to obtain quasi-steady states promptly so as to minimize memory effects, we have used 6-min periods of perturbation of $\Delta\psi$ [16, 27, 30]. Our reason for this choice was that, with the O_2 electrode system employed, a perturbation for 4 min was required to achieve a constant slope of O_2 tension versus time, and an additional 2 min was necessary in order to measure the slope accurately. Since this protocol resulted in near-linear voltage dependencies of both current and O_2 consumption we felt that we had succeeded in establishing suitable quasi-steady states, permitting the evaluation of rate-limiting parameters under circumstances in which they remained approximately constant. Recently it has been suggested that in order to achieve true steady states of both transport and metabolism, justifying their combined analysis, it is necessary to maintain voltage perturbations for periods of some 20–40 min [13].

This issue may be usefully re-examined by means of the apparatus used in the present study, which permitted monitoring oxidative metabolism with a greater degree of temporal detail than previously available to us. As shown above, we found that, following equilibration at short-circuit, on hyperpolarizing membranes to 100 mV the effect on metabolism was biphasic. Thus, to within the accuracy permitted by the noise of our system, measurements of CO_2 production demonstrated an initial quasi-steady state commencing on the average within about 3 min and lasting about 4 min, followed by further relaxation to a stable steady state commencing at about 15 min. Although less precise, a few studies of O_2 consumption gave the same qualitative result. The present results seem to us therefore to support the validity of our standard protocol, in which we usually evaluate the voltage-dependence of metabolism 4–6 min following perturbation of $\Delta\psi$ over a range of some 0 to ± 80 mV. Although measurements after 15 min would show longer periods of stability, this is not a significant advantage, since as mentioned the rate of metabolism can be accurately measured within 2 min, either with O_2 electrodes or with the apparatus used here. Furthermore, prolonged perturbations seem very likely to induce significant changes in system parameters, as indicated by nonlinear voltage dependencies of current and metabolism and by hysteresis [13, 30, 32].

In order to use the present data to characterize the formal relationships between rates of transport and O_2 consumption, it is necessary to assume that during periods of near-constancy of I and J_r the amiloride-sensitive current I^a is equivalent to the rate of active Na transport J^a_{Na}, i.e. the net rate of Na transport across the basal-lateral membrane. This has been shown to be so 10 to 20 min following commencement of bidirectional Na^+ tracer fluxes, both in the presence and absence of short-circuit [31]. Although this equivalence cannot be assumed immediately following a perturbation of the rate of transport, it seems likely to be the case during the early plateau period, following which changes in I are minimal. Thus working with frog skins, Dörge and Nagel found that on depression of short-circuit current with amiloride Na unidirectional influx and

net flux reached new steady-state values with a half-time of 3.3 min [8]. Much of this delay likely occurred following transcellular active transport, since subsequent tracer wash-out studies showed that the fast component of corial wash-out associated with active transport commenced only about 2 min after cessation of epithelial loading [21]. Such delay of onset of wash-out has been observed also by others, and presumably reflects transport through intercellular spaces and/or corial connective tissue [11]. In recent studies employing intracellular microelectrodes it has been found that following transepithelial voltage clamping the intracellular electrical potential reaches a steady-state level within some 4 min or less (Nagel and Essig, *manuscript in preparation*). In the toad urinary bladder Finn and Rockoff have reported rate constants similar to those found in the studies cited above [9].

Presuming that the rate of active Na transport is indeed near constant and given by I^a/F during the early plateau period, it is valid to use the values of I^a and J_r^{sb} to characterize the early quasi-steady state. It is then of interest to examine the behavior of J_{Na}^a/J_r^{sb}, the number of equivalents of Na^+ transported per mole of suprabasal O_2 consumed or CO_2 produced. The present results indicate that even in a given tissue there is no unique stoichiometry for this relationship, since the ratio declines markedly on changing $\Delta\psi$ from zero to $+100$ mV. This finding conforms with earlier observations from our laboratory indicating that in terms of a formal phenomenological treatment [12] Na transport and oxidative metabolism in the toad urinary bladder are incompletely coupled [16]. This finding does not of course have any specific mechanistic implications. Possible causes of uncoupling are, in principle, numerous, and have been discussed elsewhere [5, 15, 16, 26]. Since the efficiency of energy conversion is a sensitive function of the degree of coupling [12], there may be a tendency to assume that maximal *in vivo* values are optimal, and that any significant uncoupling measured *in vitro* is likely to be an artifact of the experimental preparation. In studies of mitochondrial oxidative phosphorylation, however, Stucki has pointed out that a system may operate so as to optimize functions other than energy conversion; thus there may possibly be biological advantages to a slight degree of uncoupling [29]. The physiological significance of the degree of coupling of epithelial active transport systems remains as yet obscure.

Two groups have reached conclusions concerning the degree of coupling different from those cited above. Labarca, Canessa and Leaf, studying Na^+ transport in the toad urinary bladder, and Beauwens and Al-Awqati, working with active H^+ transport in the turtle urinary bladder, have concluded that coupling was high [13] or near complete [3]. It is important to note, however, that in these authors' studies measurements of the flow ratios were made 20 min or longer following perturbation of $\Delta\psi$ [13] and some 10–20 min following perturbation of Δ pH [3]. Given the present demonstration of the strong time-dependence of J_{Na}^a/J_r^{sb}, we do not feel that there is any discrepancy between their observations and ours.

What then can account for the finding that with prolonged clamping of $\Delta\psi$ at 100 mV the value of J_{Na}^a/J_r^{sb} increases progressively from that measured in the early plateau period to the same level measured initially at short-circuit? Presently available information does not permit a definitive answer to this question, but two possibilities come to mind. First, slowing of ATP utilization consequent to slowing of transport, in the face of initially continuing high rates of oxidative phosphorylation might result gradually in significant increase of the [ATP]/[ADP] $[P_i]$ ratio. In time this would result in increase of J_{Na}^a and decrease of J_r^{sb}, as was observed. Increase of the phosphate potential, other factors being equal, should result also in increase of the magnitude of $\Delta\bar{\mu}_{Na}$ necessary to maintain J_{Na}^a near zero ("static head"). Thus, whereas initially at $\Delta\psi = 100$ mV the system was near static head, it gradually moves away from this state. However, as stressed by Kedem and Caplan, although the ratio of flows of an incompletely coupled system falls progressively with $\Delta\bar{\mu} > 0$, unless a system is highly uncoupled, decline in the ratio becomes experimentally demonstrable only in the vicinity of static head (*see* [12], Fig. 1). Accordingly, it might be expected that with prolonged voltage clamping at 100 mV, if static head increases appreciably above 100 mV, J_{Na}^a/J_r^{sb} might gradually relax to near its original short-circuit value. A second possibility is that over and above effects on the [ATP]/[ADP] $[P_i]$ ratio and the magnitude of static head, prolonged hyperpolarization might have important effects on kinetic factors (permeability coefficients, rate constants) of the system [32], possibly reflecting changes in the intracellular sodium pool, as well as tissue metabolite levels.

Further elucidation of the above-discussed mechanisms at the molecular level will be important for understanding of dynamic regulation *in vivo*, where a host of factors may modulate the pertinent forces and kinetic factors. Clearly, complete understanding will require combined studies of transport and intermediary metabolism with spatial and temporal detail. Such studies must await the development of more powerful techniques than are presently available.

This work was supported by Public Health Service Grant HL 14322 to the Harvard-MIT Program in Health Sciences and Technology, and Training Grant T 33AM 07053, and by National Science Foundation Grant PCM 76-23295.

We are grateful to Dr. Wolfram Nagel for comments on the manuscript.

References

1. Al-Awqati, Q., Beauwens, R., Leaf, A. 1975. Coupling of sodium transport to respiration in the toad bladder. *J. Membrane Biol.* **22**:91–105
2. Arczynska, W., Girardier, L., DeSousa, R.C. 1976. A comparative study of the effects of norepinephrine and vasopressin on Na transport and O_2 consumption in frog skin. *Pfluegers Arch.* **363**:187–191
3. Beauwens, R., Al-Awqati, Q. 1976. Active H^+ transport in the turtle urinary bladder. *J. Gen. Physiol.* **68**:421–439
4. Canessa, M., Labarca, P., DiBona, D.R., Leaf, A. 1978. Energetics of sodium transport in toad urinary bladder. *Proc. Natl. Acad. Sci. USA* **75**:4591–4595
5. Caplan, S.R., Essig, A. 1977. A thermodynamic treatment of active sodium transport. *In:* Current Topics in Membranes and Transport. F. Bronner and A. Kleinzeller, editors. Vol. 9, pp. 145–175. Academic Press, New York
6. Coggins, C.H., Maffly, R.H. 1965. A method for measuring micromolar quantities of carbon dioxide and $C^{14}O_2$ produced by transporting epithelial tissues *in vitro*. *Anal. Biochem.* **10**:266–273
7. Coplon, N.S., Steele, R.E., Maffly, R.H. 1977. Interrelationships of sodium transport and carbon dioxide production by the toad bladder: Response to changes in mucosal sodium concentration, to vasopressin and to availability of metabolic substrate. *J. Membrane Biol.* **34**:289–312
8. Dörge, A., Nagel, W. 1970. Effect of amiloride on sodium transport in frog skin. II. Sodium transport and unidirectional fluxes. *Pfluegers Arch.* **321**:91–101
9. Finn, A.L., Rockoff, M.L. 1971. The kinetics of sodium transport in the toad bladder. I. Determination of the transport pool. *J. Gen. Physiol.* **57**:326–348
10. Hong, C.D., Essig, A. 1976. Effects of 2-deoxy-D-glucose, amiloride, vasopressin and ouabain on active conductance and E_{Na} in the toad bladder. *J. Membrane Biol.* **28**:121–142
11. Hoshiko, T., Lindley, B.D., Edwards, C. 1964. Diffusion delay in frog skin connective tissue: A source of error in tracer investigations. *Nature (London)* **201**:932–933
12. Kedem, O., Caplan, S.R. 1965. Degree of coupling and its relation to the efficiency of energy conversion. *Trans. Faraday Soc.* **61**:1897–1911
13. Labarca, P., Canessa, M., Leaf, A. 1977. The metabolic cost of sodium transport in toad urinary bladder. *J. Membrane Biol.* **32**:383–401
14. Lahav, J., Essig, A., Caplan, S.R. 1976. The thermodynamic degree of coupling between metabolism and sodium transport in frog skin. *Biochim. Biophys. Acta* **448**:389–392
15. Lang, M.A., Caplan, S.R., Essig, A. 1977. Sodium transport and oxygen consumption in toad bladder. A thermodynamic approach. *Biochim. Biophys. Acta* **464**:571–582
16. Lang, M.A., Caplan, S.R., Essig, A. 1977. Thermodynamic analysis of active sodium transport and oxidative metabolism in toad urinary bladder. *J. Membrane Biol.* **31**:19–29
17. Lau, Y.T., Lang, M.A., Essig, A. 1979. Evaluation of the rate of basal oxygen consumption in the isolated frog skin and toad bladder. *Biochim. Biophys. Acta* **545**:215–222
18. Leaf, A., Anderson, J., Page, L.B. 1958. Active sodium transport by the isolated toad bladder. *J. Gen. Physiol.* **41**:657–668
19. Macknight, A.D.C. 1977. Contribution of mucosal chloride to chloride in toad bladder epithelial cells. *J. Membrane Biol.* **36**:55–63
20. Macknight, A.D.C. 1977. Epithelial transport of potassium. *Kidney Int.* **11**:391–414
21. Nagel, W., Moshagan, D. 1978. Wash out characteristics of tracer Na from the transport pool of frog skin. *Pfluegers Arch.* **374**:235–241
22. Nellans, H.N., Finn, A.L. 1974. Oxygen consumption and sodium transport in the toad urinary bladder. *Am. J. Physiol.* **227**:670–675
23. Noé, G., Michotte, A., Crabbé, J. 1977. Oxygen consumption by frog skin and its isolated epithelial layers as a function of their sodium transporting activity. *Biochim. Biophys. Acta* **461**:231–238
24. Owen, C.S., Wilson, D.F. 1974. Control of respiration by the mitochondrial phosphorylation state. *Arch. Biochem. Biophys.* **161**:581–591
25. Rosenthal, S.J., King, J.G., Essig, A. 1979. Use of mass spectrometer to measure CO_2 and O_2 fluxes in voltage-clamped epithelia. *Am. J. Physiol.* **236**:F413–418
26. Rottenberg, H., Essig, A., Caplan, S.R. 1967. Stoichiometry and coupling: Theories of oxidative phosphorylation. *Nature (London)* **216**:610–611
27. Saito, T., Essig, A., Caplan, S.R. 1973. The effect of aldosterone on sodium transport in the frog skin. *Biochim. Biophys. Acta* **318**:371–382
28. Snedecor, G.W., Cochran, W.G. 1967. Statistical Methods. Iowa State University Press, Ames, Iowa
29. Stucki, J.W. 1980. The optimal efficiency and the economic degrees of coupling of oxidative phosphorylation. *Eur. J. Biochem.* **109**:269–283
30. Vieira, F.L., Caplan, S.R., Essig, A. 1972. Energetics of sodium transport in frog skin. II. Effects of electrical potential on oxygen consumption. *J. Gen. Physiol.* **59**:77–91
31. Wolff, D., Essig, A. 1977. Kinetics of bidirectional active sodium fluxes in the toad bladder. *Biochim. Biophys. Acta* **468**:271–283
32. Wolff, D., Essig, A. 1980. Protocol-dependence of equivalent circuit parameters of toad urinary bladder. *J. Membrane Biol.* **55**:53–68

Received 19 November 1980; revised 20 April 1981